The Era of Multi-Messenger Solar Physics
Proceedings IAU Symposium No. 372, 2023
G. Cauzzi & A. Tritschler, eds.
doi:10.1017/S174392132300087X

Study of Ionospheric behaviour during the intense geomagnetic storms in 24th solar cycle over different Latitudes and Longitudes

Bhupendra Malvi[1], Sharad C. Tripathi[2] and P. K. Purohit[3]

[1]Department of Electronics, Barkatullah University, Bhopal - 462026, M.P., India

[2]School of Advanced Sciences and Languages (SASL), VIT Bhopal University, Bhopal - Indore Highway, Kothri Kalan, Sehore - 466114, M.P., India

[3]Department of Applied Sciences, NITTTR, Shamla Hills, Bhopal - 462003, M.P., India

Abstract. An analysis of geomagnetic disturbances and global ionospheric electron density perturbations during the 2015 St. Patrick's Day geomagnetic storm is presented in this paper. GPS observations from worldwide IGS stations are used and analysed through GPS-TEC analysis application developed by Gopi Seemala to get VTEC profiles. The St. Patrick's geomagnetic storm covers the interval of 15-23 March 2015, when transient solar eruptions (a prolonged C9-class solar flare and associated CMEs on 15 March) and a strong geomagnetic storm during 16-18 March (Dst dropped to -223 nT) were reported. This geomagnetic storm led to complex effects on the ionosphere. The global maps have been created after analysing VTEC profiles at Low, Mid and High-latitudes over different longitudinal sectors. Major features of the positive and negative ionospheric storm development are observed in Asian, European and American Low, Mid and High-latitudes.

Keywords. Geomagnetic Storm, Total Electron Content, Ionospheric Perturbations, St. Patrick's Day

1. Introduction

The biggest geomagnetic storm of the 24th solar cycle occured in the middle of March 2015 with the value of Dst index at -223 nT. It was named as the "St Patrick's Day" storm due to the occurence of its main phase on 17 March. This storm was associated with a Coronal Mass Ejection occured on 15 March 2015. SOHO/LASCO C3 recorded this partial halo CME and an associated C class solar flare was observed which erupted from the active region located at S22W25. A series of type II/IV radio bursts were also observed. It is well known that the ionospheric electric field disturbances that are observed in the medium and low latitude regions during a magnetic storm have different timescales and originate from the direct penetration of the magnetospheric electric field into the ionosphere (Nishida 1968; Vasyliunas 1970; Jaggi & Wolf 1973; Fejer et al. 1990). Magnetospheric, ionospheric and atmospheric changes during geomagnetic storms are fundamentally dynamic, interactive and nonlinear which can be represented by variations in key parameters, such as ionospheric electron densities, total electron content, electromagnetic field and currents, particle precipitation etc. The essential physical processes that can explain these coupled interactions are known only up to a certain degree, with several qualitative explanations. However, the relative importance varies from case to case establishing different storm time responses in the geospace (Zhang et al. 2017).

The present study is the first of its kind, where the ionospheric perturbations during the St. Patrick's Day storm of 17 March 2015 (which has a long-lasting main phase with

Table 1. List of the used IGS Stations.

IGS Stations					
Southern Hemisphere			Northern Hemisphere		
Lat	Long	Station Code	Lat	Long	Station Code
−77.83	166.66	MCM4	0.35	9.67	NKLG
−69	39.58	SYOG	5.25	307.19	KOUR
−68.57	77.97	DAV1	12.14	273.75	MANA
−66.28	110.51	CAS1	13.02	77.57	IISC
−64.77	295.94	PALM	13.43	144.8	GUUG
−63.32	302.09	OHI3	13.73	100.53	CUSV
−53.13	289.12	PARC	20.7	203.74	MAUI
−49.35	70.25	KIT3	21.85	257.71	INEG
−43.73	183.38	CHTI	30.59	34.76	RAMO
−37.82	144.97	MOBS	32.64	343.09	FUNC
−34.9	302.06	IPGS	35.14	33.39	NICO
−32.38	20.81	SUTH	35.95	140.65	KSMV
−31.86	133.8	CEDU	36.13	138.36	USUD
−29.04	115.34	YAR2	37.74	334.33	PDEL
−27.125	250.65	ISPA	39.02	283.17	GODZ
−25.89	27.68	HRAO	42.99	74.75	CHUM
−22.57	17.08	WIND	48.13	240.31	BREW
−20.27	289.86	IQQE	59.57	150.77	MAG0
−19.26	147.05	TOW2	60.53	29.78	STVL
−19.07	190.07	NIUM	60.75	224.77	WHIT
−12.93	321.56	SAVO	64.13	338.04	REYK
−12.18	96.83	COCO	64.26	344.81	HOFN
			64.97	212.5	FAIR
			69.36	88.35	NRIL
			71.63	128.86	TIXI
			74.69	265.1	RESO

the Dst as low as -223 nT), have been analysed all over the globe, altogether. Strong equatorial zonal electric field enhancement were observed due to two strong prompt penetration electric field phases during the main phase of this storm. The first one occured around 1200 UT with the southward IMF Bz and the second one around 1725 UT with the onset of a substorm. The enhanced electric field due to this prompt penetration of electric field lead to the strong super fountain effect (Venkatesh et al. 2017). The consequent spatiotemporal disturbances in the ionospheric TEC profile becomes more important to be investigated.

2. Datasets and Methodology

In the present analysis GPS data from various IGS stations, located around the globe, have been downloaded from Scripps Orbit and Permanent Array Center (SOPAC) website http://sopac.ucsd.edu/ and analysed using GPS-TEC analysis software developed by Gopi Seemala [http://seemala.blogspot.com/2017/09/gps-tec-program-ver-295.html to get VTEC (Vertical Total Electron Content), which is the vertically integrated electron density at a particular location at a particular time, profiles. Dst index data were downloaded from World Data Center (http://wdc.kugi.kyushu-u.ac.jp). Geomagnetically quiet days were identified from World Data Center repository and the respective GPS data were downloaded for the said IGS stations. One day VTEC profile was generated from these quiet day observations by taking standard deviations of respective observational instants on these days. This prepared data (3-sigma) was used as background and subtracted from the VTEC profiles of disturbed days; during 15-23 March 2015. Peak values on the said days, for all the IGS stations, are used to create global TEC maps. The list of IGS stations considered in present analysis are listed in table 1.

https://doi.org/10.1017/S174392132300087X Published online by Cambridge University Press

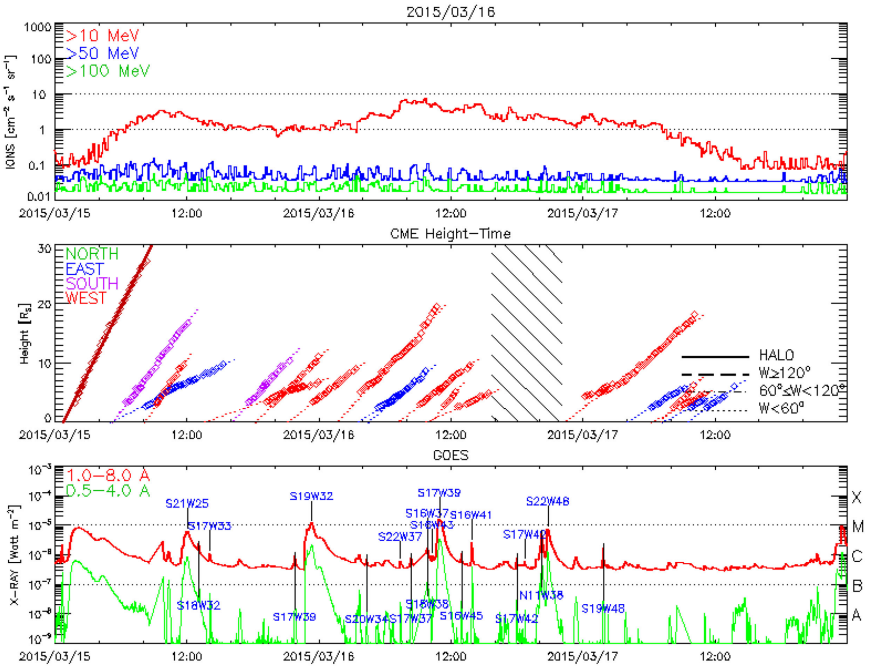

Figure 1. Solar Transients associated to St. Patrick's Day Geomagnetic Storm.

3. Results and Discussion

An intense geomagnetic storm was observed on March 17, 2015 having Dst as strong as -223 nT at 10:00 hours UT. A total of 48 stations were identified, from all over the globe, for which GPS data was availabile during the observational window 15-23 March 2015. These stations were selected for analysing ionospheric perturbations in various longitudinal and latitudinal regions; represented as grids in the figure 3. Several solar transients were observed before the main St. Patrick's Day event, and are possibly associated with it, see figure 1 [Source: `https://cdaw.gsfc.nasa.gov/`]. Dst data downloaded from World Data Center repository is plotted in figure 2. Global VTEC profiles are shown in figure 3 where daily background corrected peak values are plotted in the various grids of subplots (from a to i). In the 0°-30°E longitude range it is observed that the TEC is increased in the equatorial and mid latitude regions of southern hemisphere during the main phase of geomagnetic storm. In the 30°E-60°E longitude range peak values of background corrected daily VTEC profiles are plotted in the global TEC maps and it is observed that the TEC was increased everywhere, except at the high latitude station in southern hemisphere, during the main phase of the geomagnetic storm. In the 60°E-90°E longitude range it is observed that the TEC decreased everywhere during the main phase of the geomagnetic storm. In the 90°E-120°E longitude range it is observed that the TEC decreased everywhere during the main phase of the geomagnetic storm. In the 120°E-150°E longitude range it is observed that the TEC decreased everywhere during the main phase of the geomagnetic storm. In the 150°E-180° longitude range it is observed that the TEC increased everywhere during the main phase of the geomagnetic storm. In the 150°W-180° longitude range it is observed that the TEC decreased, except at the equatorial station in the southern hemisphere, during the main phase of the geomagnetic storm. In the 120°W-150°W longitude range it is observed that the TEC increased, except at the higher latitude station in northern hemisphere, during the main phase of the geomagnetic storm and decreased during the recovery phase. Equatorial region stations in both the

https://doi.org/10.1017/S174392132300087X Published online by Cambridge University Press

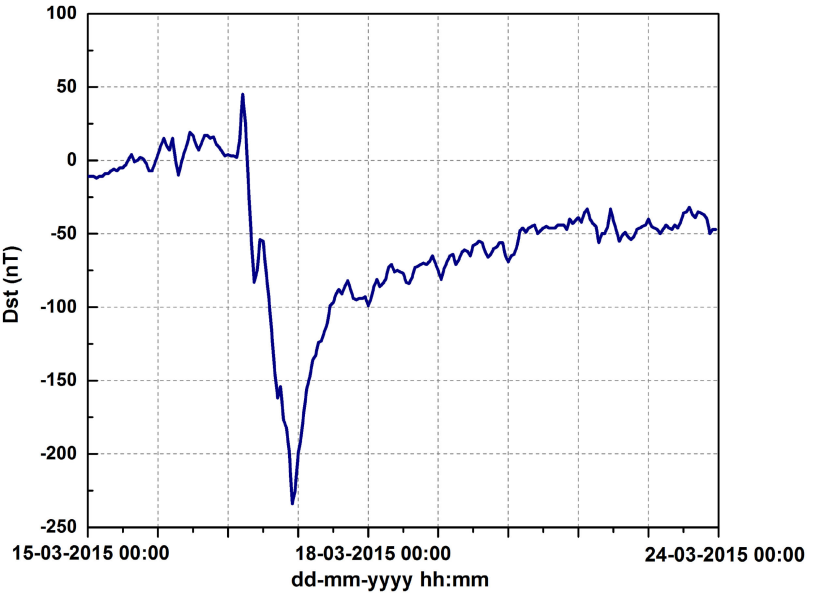

Figure 2. Dst variations during St. Patrick Day Geomagnetic Storm.

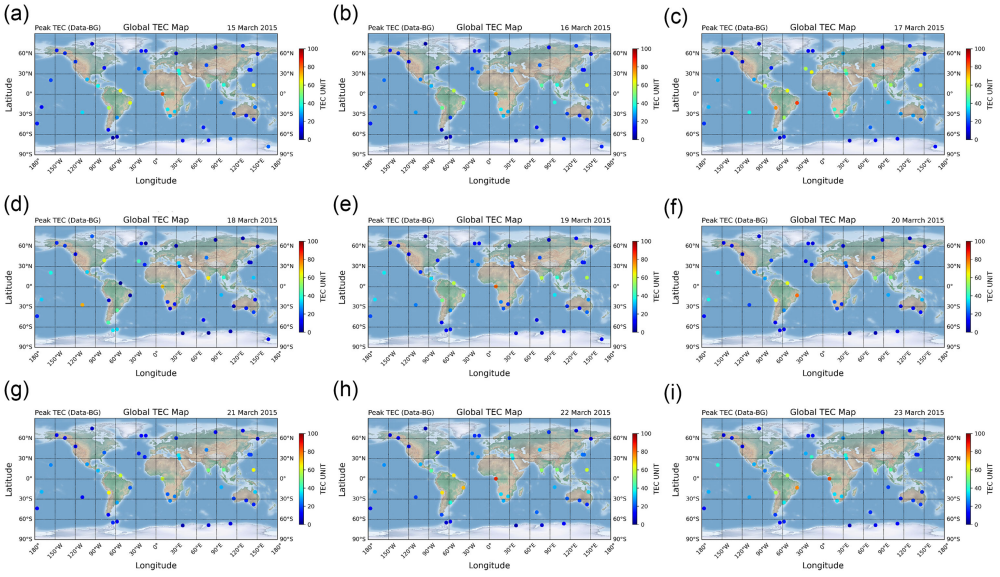

Figure 3. Global Ionospheric responses during St. Patrick's Day Geomagnetic Storm.

hemispheres and Mid latitude station in the southern hemisphere witnessed most prominent disturbance during the main phase of geomagnetic storm, whereas, the mid latitude station in the northern hemisphere got delayed response, ionospheric TEC increased here, next day. In the 90°W-120°W longitude range it is observed that the TEC increased, except for the higher latitude station in northern hemisphere, during the main phase of the geomagnetic storm and decreased during the recovery phase. Mid latitude station in both the northern and southern hemisphere witnessed most prominent disturbance during the main phase of geomagnetic storm. In the 60°W-90°W longitude range it is observed that the TEC increased during the main phase of the geomagnetic storm and

https://doi.org/10.1017/S174392132300087X Published online by Cambridge University Press

decreased during the recovery phase. Mid latitude station in the northern hemisphere witnessed most prominent disturbance during the main phase of geomagnetic storm. In the 30°W-60°W longitude range it is observed that the TEC increased during the main phase of the geomagnetic storm, in the equatorial region and higher latitudes of southern hemisphere. In the 0°-30°W longitude range it is observed that the TEC increased during the main phase of the geomagnetic storm, in the mid latitude and higher latitudes regions of northern hemisphere.

4. Conclusions

Global ionospheric perturbations in VTEC profiles at various longitudinal regions reflect delayed effects at some locations, somewhere it is positive and somewhere it is negative, due to the complex geomagnetic responses. The interaction of the Solar Plasma at geospace and the storm preparation is believed to plays a key role in such complex disturbances.

Acknowledgements

Author Bhupendra Malvi is thankful to the International Astronomical Union (IAU) for providing a grant for his participation in IAUGA 2022 hosted at BEXCO in Busan, Republic of Korea during August 2-11, 2022.

References

Fejer, B., Spiro, R., Wolf, R., & Foster, J. 1990, Geophysical Journal;(France), 8

Jaggi, R. K. & Wolf, R. A. 1973, Journal of Geophysical Research (1896-1977), 78, 2852

Nishida, A. 1968, Journal of Geophysical Research (1896-1977), 73, 5549

Vasyliunas, V. M. 1970, in Particles and Fields in the Magnetosphere, ed. B. M. McCormac (Dordrecht: Springer Netherlands), 60–71

Venkatesh, K., Tulasi Ram, S., Fagundes, P. R., Seemala, G. K., & Batista, I. S. 2017, Journal of Geophysical Research: Space Physics, 122, 4553

Zhang, S.-R., Zhang, Y., Wang, W., & Verkhoglyadova, O. P. 2017, Journal of Geophysical Research (Space Physics), 122, 6901